



Cite this: *Environ. Sci.: Water Res. Technol.*, 2023, 9, 1654

Low-irradiance inactivation kinetics of *Escherichia coli* during prolonged exposure to ultraviolet-C radiation

Muhammad Salman Mohsin, Katrina Fitzpatrick, Melisa Avdic, Joshua Fiorentino and Mariana Lanzarini-Lopes *

There is growing interest in using continuous, low-irradiance germicidal ultraviolet (UV) radiation to prevent bacterial attachment, growth, and biofilm formation on surfaces through water distribution pipes, appliances, and point-of-use plumbing. This study explored the low irradiance dose response of surface-bound *Escherichia coli* (*E. coli*). A linear model was used to calculate the pseudo-first-order inactivation rate constant (k'), and a minimum irradiance ($\mu\text{W cm}^{-2}$) was established to achieve inactivation of surface-bound organisms in a nutrient-rich environment. The k' for irradiance above $0.21 \mu\text{W cm}^{-2}$ was calculated to be $1.06 \pm 0.05 \text{ cm}^2 \text{ mJ}^{-1}$. The kinetic model reveals that UV irradiance above $0.21 \mu\text{W cm}^{-2}$ can result in up to 6 log inactivation at a dose of $<6.0 \text{ mJ cm}^{-2}$. The minimum UV irradiance required for complete inactivation of surface-bound *E. coli* during prolonged exposure was averaged to be $0.38 \pm 0.11 \mu\text{W cm}^{-2}$ and $0.18 \pm 0.02 \mu\text{W cm}^{-2}$ for 265 nm and 280 nm wavelength, respectively. This study provides new knowledge and guidance to design technologies for disinfecting surfaces and a control strategy for biofilm prevention with very low UV irradiance ($\mu\text{W cm}^{-2}$).

Received 21st November 2022,
Accepted 28th March 2023

DOI: 10.1039/d2ew00886f

rsc.li/es-water

Water impact

There is increased interest in using UV light for pathogenic biofilm prevention in enclosed water channels and pipes. However, there is no consensus on a minimum UV flux needed to sustain passive treatment. The findings in this research will directly impact the development and design of UV technologies for inactivation of bacteria on surfaces.

A. Introduction

Biofilms can easily attach and grow on wetted surfaces such as water distribution pipes, appliance channels (e.g., refrigerators/coffee makers), and point-of-use plumbing.^{1,2} Early-stage biofilms begin to form during initial contact between microorganisms and a surface in water and can grow into complex biofouling communities within days.¹ These biofilms grow into dense biomass ranging from micrometers to millimeters in thickness, harbor pathogenic bacteria, and can contaminate clean drinking water.³⁻⁵ Additionally, biofilms can create acid metabolites that corrode water distribution pipes (metallic and concrete) and cause hydraulic pressure drops throughout the conduit.⁶ Current biofilm prevention strategies for water distribution pipes include (i) treating and disinfecting the water before

distribution and (ii) maintaining a disinfection residual through water use.⁷ However, leakage into the water distribution system introduces new nutrients and microbiological communities into the plumbing. It only takes a few organisms attached to a surface to begin forming complex biofilm structures.

There is growing interest in implementing UV light for continuous exposure on surfaces of point-of-use tubing, piping, and showerheads to prevent biological growth and infection of the consumer.⁸⁻¹¹ UVC radiation between 240 and 280 nm is categorized as germicidal because it inhibits pathogens (i.e., bacteria, viruses, protozoa) from replicating and infecting a host.^{12,13} Absorption of UV light by nucleic acids results in crosslinking between thymine and cytosine. These mutations disable hydrogen bonding to the opposite strand's purine base, inhibiting replication.¹⁴ The amount of crosslinked pyrimidine nucleotide bases is directly related to UV exposure.

UV light-emitting diodes (LEDs) are attractive in water treatment due to lack of mercury or warm-up time, specific

Environmental and Water Resources Engineering, Department of Civil and Environmental Engineering, University of Massachusetts Amherst, MA, 01003, USA.
E-mail: marianalopes@umass.edu



wavelength emission, no degradation from on/off cycles, high durability, and long-term use.^{9,10,15–20} The compact nature of LEDs allows engineers to explore new designs for point-of-use (POU) disinfection applications.²¹ These LEDs can be placed in sinks, storage units, water bottles, and point-of-use water treatment. UV LEDs are also gaining traction for their potential to disinfect showerheads and distribution systems. Cates and Torkzadeh proposed a showerhead design with LEDs to prevent opportunistic respiratory pathogens from infecting immunocompromised individuals.²² Lanzarini-Lopes *et al.* previously illustrated how UV side-emitting optical fibers can be used to guide light from UV LEDs into tight enclosed channels.^{23,24} Linden *et al.* depicted a vision for UV secondary disinfection that takes advantage of the LED geometry to distribute light throughout the water distribution system.²⁵ In these applications, UV light would serve as both the last barrier and the residual disinfectant to inactivate microbial pathogens released from pipes during the distribution of treated water. This vision would prevent (i) operational problems and (ii) health hazards associated with the growth of pathogenic organisms in piping.

However, there is a large knowledge gap in trying to use UV light in applications where a surface would be exposed to UV light for a prolonged time. In this context, we define prolonged as greater than 12 h to indefinite, where the light source would remain on continuously until it is replaced. Traditionally, the dose is the primary design parameter for disinfection because time is usually the limiting variable for both batch and flow-through reactors when using high-power lamps. The literature until 2020 reported the UV dose ($J\text{ cm}^{-2}$) required for the inactivation of organisms, where dose ($J\text{ cm}^{-2}$) = exposure time (s) \times UV irradiance ($W\text{ cm}^{-2}$). Unlike flow-through or batch reactions that expose water to UV light for seconds to minutes, prolonged UV light exposure on surfaces can result in a very high (infinite) UV dose. Therefore, the ultraviolet irradiance ($W\text{ cm}^{-2}$) becomes the limiting variable and can be insufficient to either (i) damage the DNA and protein of the organism or (ii) surpass the rate of DNA and protein reconstruction.²⁶ There is a need to understand the minimum UV irradiance required to inactivate organisms during prolonged surface exposure.

Recently, Torkzadeh *et al.* illustrated that at least $50.5\text{ }\mu\text{W cm}^{-2}$ was needed to reduce the biovolume by 95% in a highly fouling environment.²⁷ The authors eloquently described the importance of the work, proposed a method that can be used to assess the irradiance response, and recommended a minimum irradiance needed for biofilm prevention in showerheads. In this study, we explored a similar idea of using low intensity UV-C irradiation for biofilm prevention. Specifically, this work focuses on inactivation of surface-bound organisms in a nutrient-rich environment before they begin forming complex biofilm structures. To our knowledge, no work has explored the low irradiance ($<1\text{ }\mu\text{W cm}^{-2}$) dose response in surface-bound *E. coli*. This work seeks to quantify the pseudo-first-order kinetics of inactivation during prolonged ($>18\text{ h}$) low irradiance conditions, establish a

minimum irradiance needed to achieve inactivation of surface-bound organisms in a nutrient-rich environment, and propose a method of calculating an energy budget for a surface bound UV disinfection system.

B. Materials and methods

Bacterial cultivation

E. coli was used as the indicator microorganism²⁸ to study low UV-C irradiance inactivation efficiency at different irradiance and exposure times. A pure culture of an *E. coli* strain (ATCC 25922) was used, and $100\text{ }\mu\text{L}$ of the generation zero bacteria was added to 25 ml of tryptic soy broth (TSB) in a centrifuge tube and placed on a shaker table (140 rpm) inside an incubator at $37\text{ }^\circ\text{C}$ for 18 to 24 hours. The overnight culture was mixed with 50% by volume glycerol solution in a 1:1 ratio and then aliquoted into microcentrifuge tubes and stored in a $-80\text{ }^\circ\text{C}$ freezer to be used as culture stock.²⁹

The generation one culture was prepared by mixing a 1:10 ratio of the culture stock and TSB. Following overnight (18–24 h) incubation, the culture was diluted in a 1:10 ratio with TSB, incubated ($37\text{ }^\circ\text{C}$), and mixed (140 rpm) for 2 hours to achieve an optical density (OD) of 1 cm^{-1} (10^8 cells per ml).²⁹ A UV-Vis spectroradiometer was used to measure the OD. The culture was washed three times by centrifuging (4000 rpm , 1 min) in a phosphate buffer solution (PBS). Washing is necessary to avoid UV absorption by broth media during UV experiments. Agar plates were used throughout the experiment during irradiation and for quantifying colony-forming units (CFU). The agar plates were prepared by mixing 10 g tryptic soy agar (TSA) (2291, Sigma-Aldrich) in 250 ml of liquid broth media and then autoclaved for 20 min at $121\text{ }^\circ\text{C}$. Approximately, 50 ml of solution was poured into a 15 cm diameter round polystyrene petri dish and cooled.

To quantify the density of *E. coli* in the initial solution, a volume of $50\text{ }\mu\text{L}$ of serially diluted samples were evenly spread on tryptic soy agar (TSA) plates and incubated at $37\text{ }^\circ\text{C}$ for 18 to 24 hours. Colony forming units (CFU) were counted *via* the plate streaking technique.³⁰

Quantification of the inactivation rate constant during low irradiance exposure

To quantify *E. coli* inactivation by low 265 nm UV irradiance, a 3 cm^2 Pearl Lab Micro™ UV chamber (AquiSense Technologies) equipped with a 265 nm UV LED was modified to enable uniform scattering of irradiance across the agar plate surface (Fig. 1-A). The chamber was operated at the lowest power setting, and the agar plates were covered with (1–4) UV translucent films (UVT $\sim 27\%$) to decrease the incident irradiance further.

The incident irradiance was measured using a spectroradiometer (AvaSpec-ULS2048CL-EVO) (minimum detection = $0.10\text{ }\mu\text{W cm}^{-2}$). Readings lower than the minimum detection were quantified linearly by measuring absorption by the UV translucent film explained earlier. In





Fig. 1 Schematic of (A) the UV dome used for quantifying the dose–response constant during low UV irradiance exposure and (B) the UV-C LED set up for obtaining minimum irradiance needed for inactivation during prolonged exposure.

this experimental set up, the spectroradiometer sensor tip (3.9 mm) was placed parallel to the UV-C LED with a separation distance the same as that of the agar plate (3 cm) in the UV reactor to measure the light distribution profile of the reactor. Total irradiance was calculated by integrating the output light spectrum from the spectroradiometer from 240 nm to 300 nm. There was a $\sim 26.6\%$ drop in irradiance around the edges of the UV reactor. All light intensity measurements were taken in open air on an optical table. A 15 cm gap was used between the optical tabletop and the sensor tip to eliminate reflection interference from the optical table.

A volume of 50 μL of serially diluted *E. coli* was spread on pre-prepared agar plates. A culture of approximately 10^6 CFU cm^{-2} of *E. coli* was exposed to continuous low UV-C radiation of $0.02 \mu\text{W cm}^{-2}$, $0.06 \mu\text{W cm}^{-2}$, $0.21 \mu\text{W cm}^{-2}$ and $0.78 \mu\text{W cm}^{-2}$ for intervals of 1 h, 3 h, 6 h, 12 h and 24 h each. The exposure took place inside an incubator chamber at 37°C . Only plates with a CFU count of 30 to 300 were used for analysis. After exposure, the plates were incubated for 18 to 24 h before counting CFU. The experiments were run in independent random time series with duplicates for each time point. Finally, a linear empirical model (eqn (1)) was used to quantify the pseudo-first-order UV inactivation rate constant (k') at a low UV dose (D).

$$\text{Log inactivation} = \log_{10}\left(\frac{N_0}{N}\right) = k'D \quad (1)$$

Statistical analysis. Two sample *t*-tests were performed to determine the statistical significance between the dose response curves at each irradiance explored in this study. The standard error (SE) and R^2 of the pseudo-first-order UV inactivation rate constant (k') in eqn (1) were calculated using the linear regression function in OriginPro 2021 with the intercept fixed at zero.

Minimum UV irradiance quantification for 265 nm and 280 nm wavelengths

UV exposure. The minimum UV irradiance for prolonged exposure was explored at both 265 and 280 nm. A UV LED

was placed adjacent to an agar plate and elevated by 1 cm as shown in Fig. 1-B. Three 25 μL aliquots of *E. coli* culture were spread in the form of a streak across the agar plate. The number of bacteria per unit area in each bacterial streak was approximately 825 000 per cm^2 . There was an exponential decrease in incident UV irradiance on the agar plate, and therefore incident on the bacterial colonies, with distance from the LED. The streak began 4.8 cm away from the UV-C LED to account for the natural Lambertian profile of UV LEDs. The central streak was aligned with the center of the UV-C LED, while the adjacent streaks were offset by 2.5 cm on both sides. The experimental apparatus was placed in a biosafety cabinet to avoid contamination. After 18 to 24 h of UV exposure, the samples were incubated in a temperature room at 37°C for 24 h before analysis. Finally, the distance between bulk *E. coli* growth and the LED was measured as shown in Fig. 3-A. Single CFUs with a gap of more than 0.5 cm from the adjacent CFU were considered anomalous and not accounted for in measuring the minimum irradiance required for complete inactivation. The incident irradiance was calculated based on the distance of the start of the continuous cells from the LED and averaged for all three bacterial streaks. Independent triplicates were conducted, resulting in nine replicate measurements. A dark control (no UV exposure) was measured for comparison to the UV-C exposed samples.

Irradiance measurements. The minimum irradiance ($\mu\text{W cm}^{-2}$) needed for log inactivation was measured using a spectroradiometer. The incident irradiance was measured per cm along the surface of the bacterial streaks from 0 to 7 cm by facing the stfgap241 cm below the UV-C LED (Fig. 1-B). Triplicate measurements were taken at each position to eliminate vibrational measurement error. Fig. 3-A shows an exponential decrease in incident irradiance with increased distance from the LED. A UV profile model fit was established for each LED and streak position.

Establishing an energy budget for UV technologies

In any light-based disinfection system, the electrical energy affects the operating cost of the technology. Calculating the electrical energy required for 1 log inactivation allows us to establish an energy budget and understand the operating



cost of the technology. In bulk water treatment, this value is defined as the electrical energy required to reduce the concentration of a pollutant by one order in 1 m³ volume of water.⁹ For surface disinfection, we have defined $E_{P,N}$ as the electrical power required for 1 log inactivation per 1 cm² of surface assuming perfect light distribution from the source to the surface as described by eqn (2), where F_N is the fluence rate required for N log reduction (W cm⁻²) and C is the wall-plug efficiency of the light source.

$$E_{P,N} = \frac{F_N}{C} \quad (2)$$

This value can be used to calculate an energy budget for a surface by knowing the surface area that requires inactivation (A_s) and the light source distribution efficiency (η_D). The distribution efficiency is the fraction of light incident on the surface of interest (higher than the minimum required irradiance) divided by the total light emitted by the LED. The distribution efficiency and energy budget are relevant for the final design of a surface disinfecting system.

$$EB = \frac{(A_s F_N)}{(C \eta_D)} \quad (3)$$

C. Results and discussion

Low UV irradiance inactivation dose response at 265 nm wavelength

Fig. 2 shows the UV dose response at each irradiance (0.02 $\mu\text{W cm}^{-2}$, 0.06 $\mu\text{W cm}^{-2}$, 0.21 $\mu\text{W cm}^{-2}$ and 0.78 $\mu\text{W cm}^{-2}$). A linear model was used to calculate k' (pseudo-first-order inactivation rate constant) before achieving maximum inactivation (6 log inactivation) as per our methods of analysis. Above 0.21 $\mu\text{W cm}^{-2}$, the UV dose response follows statistically similar inactivation kinetics and there was no statistically significant difference ($p > 0.05$, unpaired t -test) in inactivation observed for 0.78 $\mu\text{W cm}^{-2}$ and 0.21 $\mu\text{W cm}^{-2}$ UV irradiance. The k' for irradiance of 0.78 $\mu\text{W cm}^{-2}$ and 0.21 $\mu\text{W cm}^{-2}$ was calculated to be $1.06 \pm 0.05 \text{ cm}^2 \text{ mJ}^{-1}$. The kinetics linear fit reveals that 6-log inactivation can be achieved with a minimum UV irradiance of 0.21 $\mu\text{W cm}^{-2}$ at $\sim 5.6 \text{ mJ cm}^{-2}$ UV dosage (Fig. 2).

The reported dose of low irradiance inactivation varies between studies for both surface and water disinfection. Table 1 shows five studies, including the current, that reported UV inactivation at UV irradiance $< 500 \mu\text{W cm}^{-2}$. Cheng *et al.* reported a comparable dose of 11.88 mJ cm^{-2} for a 5-log reduction of surface-bound *E. coli* at $39.6 \mu\text{W cm}^{-2}$ UV irradiance.²⁹ Green *et al.* and Nyangaresi *et al.* reported a dose of 7 mJ cm^{-2} and 11.52 mJ cm^{-2} for 4.88 and 4 log reduction of *E. coli* at $90 \mu\text{W cm}^{-2}$ and $384 \mu\text{W cm}^{-2}$ UV irradiance in an aqueous suspension of bacteria on a Petri dish.^{31,32} A significantly lower dose of 0.6 mJ cm^{-2} was reported for > 5 log reduction of *E. coli* at $4.24 \mu\text{W cm}^{-2}$ UV irradiance by D. K. Kim *et al.*, which is 9 times lower than

our observed results.³³ The group used a lower cell concentration of 10^5 CFU ml^{-1} in their work. The high cell density of bacteria in the outer layer of culture droplets can prevent the UV radiation from reaching the inner planktonic cells and can result in higher observed UV resistance.²⁹

The results shown in Fig. 2 supports the hypothesis that a minimum effective incident UV irradiance (W cm^{-2}) exists. There is a statistically significant distinction ($p < 0.05$, group two-sample t -test) between high (0.78 and 0.21 $\mu\text{W cm}^{-2}$) and low (0.06 and 0.02 $\mu\text{W cm}^{-2}$) dose response curves. The irradiance values of 0.06 $\mu\text{W cm}^{-2}$ and 0.02 $\mu\text{W cm}^{-2}$ do not follow pseudo-first-order kinetics. A maximum of $0.2\text{--}0.4 \pm 0.09$ log inactivation was observed for all exposure times analysed. No statistically significant difference ($p = 0.5$, unpaired t -test) in inactivation was observed for longer exposure times or between 0.06 and 0.02 $\mu\text{W cm}^{-2}$.

Irradiance below $0.06 \mu\text{W cm}^{-2}$ may not follow a general dose response due to the rate of growth or bacterial DNA repair mechanism exceeding the UV DNA destruction rate. Previous studies have shown that most photoreactivation repair takes place within the first 2 hours, and a maximum of up to 85% reactivation can be achieved.^{26,34–36} Dark repair mechanisms can lead to 25% log repair during 4 h of incubation.²⁶ However, a detailed study is needed to better understand the rate of DNA repair mechanisms at lower UV irradiance ($\mu\text{W cm}^{-2}$).

Minimum UV irradiance for prolonged exposure

The kinetic experiments narrowed the range of UV irradiance that caused an inactivation response from *E. coli*. To quantify the minimum irradiance required for inactivation in an agar plate, an 8 cm streak of bacterial inoculum was exposed to a range of UV irradiance from $2.32 \mu\text{W cm}^{-2}$ to $0.10 \mu\text{W cm}^{-2}$. Because light decays exponentially throughout the streak, it is imperative to accurately quantify the irradiance at each specific distance in the exact configuration of the experiment.



Fig. 2 UV dose response of *E. coli* at low UV intensities for 265 nm wavelength. The inset represents the non-statistically different pseudo-first-order rate constants for 0.02 and 0.06 $\mu\text{W cm}^{-2}$. The dotted line represents the combined linear fit for both intensities with a pseudo-first-order rate constant of $1.06 \text{ cm}^2 \text{ mJ}^{-1}$.



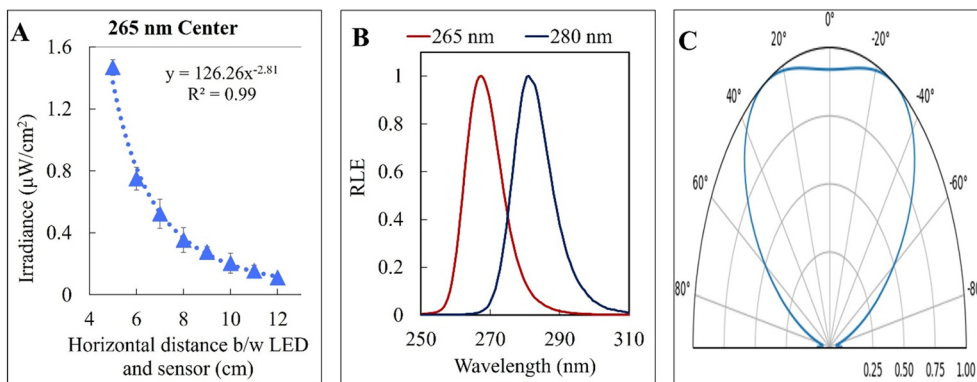


Fig. 3 (A) UV incident irradiance along the central *E. coli* inoculum streak length from the 265 nm UV-C LED. The relative lamp emission (RLE) (B) and light distribution pattern (C) of the two UV-C LEDs are also shown.

Table 1 Comparison of UV irradiance ($\mu\text{W cm}^{-2}$), wavelength (nm), dosage (mJ cm^{-2}), and log inactivation reported by various studies for different *E. coli* strains

Study	Method of culture growth	Bacterial strain	λ (nm)	Irradiance ($\mu\text{W cm}^{-2}$)	Time (min)	Dose (mJ cm^{-2})	Log inactivation
Cheng <i>et al.</i> (2020) ²⁹	Surface-bound <i>E. coli</i> in nutrient-rich media	ATCC 25922	280	39.6	5	11.88	5 log
D. K. Kim <i>et al.</i> (2017) ³³	Surface-bound <i>E. coli</i> in nutrient-rich media	O157:H7	266	4.24	2.3	0.6	>5 log
Green <i>et al.</i> (2018) ³¹	Planktonic <i>E. coli</i> in aqueous suspension	O157:H7	268	90	1.3	7	4.88 log
Nyangaresi <i>et al.</i> (2018) ³²	Planktonic <i>E. coli</i> in aqueous suspension	CGMCC 1.3373	267	384	0.5	11.52	4 log
Current study	Surface-bound <i>E. coli</i> in nutrient-rich media	ATCC 25922	265	0.21	449	~5.6	6 log

The irradiance was measured every 1 cm along the length of all three streaks perpendicular to the UV-C LED using a calibrated spectroradiometer and fit into a model to enable accurate prediction at any point of the streak. Fig. 3-A shows the decrease in incident irradiance with an increased distance from the LED.

Generally, unencapsulated LEDs are diffused and incoherent sources of light, which means that the radiation pattern emitted by the LED chip reaches maximum intensity at the angle perpendicular to the junction plane and decreases to the cosine of the angle away from the perpendicular axis. This pattern is known as the Lambertian pattern. Therefore, a combination of the inverse-square law³⁷ and Lambert's cosine law can be used to model a light distribution profile from a point source following eqn (4).

$$I_m = \frac{I_0 \cos \theta}{D^2} \quad (4)$$

However, the LEDs used in this section of the study, VPS 134 (265 nm) and VPS 164 (280 nm) from Boston Electronics, are semi-diffused sources of light with light partially focused at a 120° viewing angle (Fig. 3-C), which led the actual irradiance profile to deviate from eqn (4). Therefore, a power curve fit model was used to accurately quantify the irradiance at specific distances from the LED as shown in eqn (5), where *A* and *B* are specific fit constants.

$$Y = Ax^B \quad (5)$$

The fit constants for calculating the UV irradiance throughout each streak are listed in Table 2, along with the coefficient of determination (R^2). One example of the fit for the 265 nm LED central streak position is shown in Fig. 3-A.

The constant *A* represents the irradiance at the initial position (I_0), while *B* represents the magnitude of decay in light intensity with distance from the initial position. The variation in both intensity and magnitude of decay results from the LED intensity profile of the LED output, as shown in Fig. 3-C, in combination with the semi-diffused irradiation profile. For example, as indicated in Fig. 3-C, the intensity at a 60° angle from the center is 50% of the intensity at a 25° angle from the center. The 265 nm LED peaks at 265 nm with a 240–300 nm bandwidth. The 280 nm LED peaks at 280 nm with a 260–310 nm bandwidth. The relative (RLE) spectral profile for both LEDs is shown in Fig. 3-B.

Table 2 Power fit equation constants and R^2 values for 265 nm and 280 nm LEDs

LED	Position	<i>A</i>	<i>B</i>	R^2
265 nm	Left	220	-2.98	0.97
	Center	126	-2.81	0.99
	Right	74	-2.64	0.98
280 nm	Left	149	-2.93	0.99
	Center	167	-3.04	0.99
	Right	65	-2.69	0.99



As presented in Fig. 4, the average minimum irradiance of inactivation of surface-bound bacteria in a nutrient-rich medium resulted in $0.38 \pm 0.11 \mu\text{W cm}^{-2}$ and $0.18 \pm 0.02 \mu\text{W cm}^{-2}$ for 265 nm and 280 nm wavelengths, respectively. The irradiance is in line with a previous study by Lanzarini-Lopes *et al.* that reported a singular calculated minimum irradiance value of $0.30 \mu\text{W cm}^{-2}$ for complete inactivation of surface-bound *E. coli* at 265 nm wavelength.²⁴ Other researchers have explored the minimum irradiance required for biofilm prevention in flow-through reactors and higher-complexity environments. For example, Torzkadeh *et al.* reported an irradiance of $50.5 \mu\text{W cm}^{-2}$ needed to reduce the biovolume of biofilm by 95%.²⁷ This could be due to various reasons, such as biofilm production in the flow through cells in TSB introducing complexity to the reactor design not seen in our experimental set-up. Additionally, biofilms are much more complex than surface attached cells and include extra polymeric substances that protect the bacteria from environmental hazards. In general, we expect a high degree of variation in the response of inactivation under low irradiance conditions due to the environmental and flow conditions such as available nutrients, biofilm maturity, temperature, pH, particle count, and shading potential.^{38–41}

The electrical power per area that resulted in $>6 \log$ inactivation (no cell growth detected) was calculated and is shown in Fig. 4. The 280 nm wavelength resulted in two times lower irradiance required for complete inactivation of *E. coli* when compared to 265 nm light. Cheng *et al.* reported a similar phenomenon in which 280 nm resulted in higher inactivation of *E. coli* compared to 254 nm and 265 nm wavelengths.²⁹ Protein has a peak absorbance at 280 nm wavelength caused by aromatic

amino acids such as tryptophan and tyrosine.^{42,43} Photons absorbed by the cellular membrane protein and amino acid charge them into an excited state leading to deterioration.^{33,44} Additionally, the surface chemistry of the substrate can play a role in UV inactivation. For example, UV radiation at 280 nm can lead to a higher formation of reactive oxygen species (ROS) than that at 265 nm. The formation of reactive oxygen species (ROS) induces cellular damage like membrane destruction,³³ membrane lipid peroxidation, and respiratory enzyme activity.⁴⁵ These indirect processes can contribute to higher inactivation of *E. coli* at 280 nm wavelength and, therefore, a lower required minimum irradiance for inactivation during prolonged exposure. However, more research is needed to understand the importance of the substrate surface for UV surface disinfection.

Approximately $20.06 \pm 2.44 \mu\text{W cm}^{-2}$ and $8.02 \pm 0.91 \mu\text{W cm}^{-2}$ electrical power is required for $\geq 6 \log$ inactivation of *E. coli* for 265 and 280 nm wavelengths, respectively. In context, if 265 nm UV light was evenly distributed through the inside of a 1 m long (1 cm ID) shower hose indefinitely, it would take approximately 0.02 W power or 0.45 Wh energy per day to keep the system running. However, similar studies would have to be done with the same material of interest and flow conditions to accurately calculate the minimum UV irradiance needed for each specific application.

The electrical power required for the 280 nm wavelength LED was 2.52 times lower as compared to the 265 nm wavelength LED as calculated by eqn (2). The difference is due to (1) a lower inactivation irradiance and (2) a higher wall plug efficiency of 2.2% for the 280 nm LED as opposed to 1.8% for the 265 nm LED. Researchers and system designers should continue to explore wavelength specific mechanisms of disinfection to decrease the operating cost of UV systems (Fig. 4).

As shown in Fig. 4 (inset), singular colonies were formed inside the reported inhibition zone. The singular cells can be a result of three phenomena, including (1) the development of UV resistance, (2) inactivation after colony growth, and (3) shielding by other bacteria during UV exposure. The first two phenomena were tested by resuspending the random CFU observed inside the inhibition zone and performing similar inactivation experiments. Similar inactivation kinetics indicated that the bacteria have not developed UV resistance and were viable to reproduce under no UV exposure. Other studies previously reported the third phenomenon indicating that bacterial cells can be shielded from UV radiation during exposure and can still grow into a colony. For example, Cheng *et al.* reported that the thickness of bacterial culture droplets spread over agar plates significantly lowers the UV sensitivity of bacteria.²⁹ The higher cell density of bacteria in the outer layer of culture droplets can prevent UV radiation from reaching the inner planktonic cells and causes DNA damage. This is a much simpler yet similar mechanism to the UV shielding of cells inside biofilms that significantly inhibits the UV sensitivity of bacteria.^{38–41}

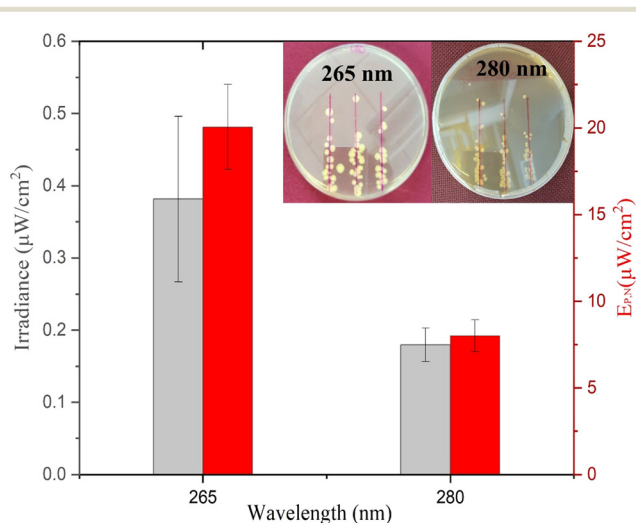


Fig. 4 Minimum irradiance ($\mu\text{W cm}^{-2}$) and electrical power per $\geq 6 \log$ inactivation of *E. coli* from exposure to UV-C LEDs at 265 nm and 280 nm wavelengths for 20 hours. The inset represents the irradiated agar plates for 265 nm and 280 nm UV-C LEDs.



Conclusions

The primary contribution of this study was quantifying the minimum irradiance required for surface inactivation of *E. coli* during prolonged exposure. This is the first study to highlight the importance of understanding the minimum irradiance when designing UV systems that take advantage of low-irradiance prolonged inactivation mechanisms. A pseudo-first-order inactivation rate constant was quantified for the inactivation of surface-bound *E. coli*. An energy budget was established for light-driven technologies seeking to apply a minimum inactivation irradiance. Finally, this study highlights that the minimum irradiance for prolonged inactivation of a surface will be dependent on wavelength. There is increased interest in using UV light for biofilm control strategies. It is, however, important to understand the distinction between biofilm inactivation and biofilm prevention. Biofilm inactivation refers to the ability to disinfect cells within an already established biofilm structure.^{46,47} Biofilm prevention refers to the ability to prevent the growth and replication on a surface that will lead to the formation of biofilms. The results lay a framework that can be used to design technologies for disinfecting surfaces and a control strategy for biofilm prevention with very low UV irradiance ($\mu\text{W cm}^{-2}$). For example, continuous low UV irradiance exposure for long periods of time can be used to suppress biofilm formation in both water distribution systems and point-of-use technologies. Running the LED at low irradiance ($\mu\text{W cm}^{-2}$) increases the LED lifetime and decreases the operational costs of treatment. Further research for various targeted microorganisms and surfaces is needed to quantify the minimum UV-C irradiance for inactivation at different wavelengths.

Conflicts of interest

There are no conflicts of interest to declare.

Acknowledgements

This work was partially funded by the National Science Foundation (NSF 21-563) and the University of Massachusetts Manning/IALS Innovation Grants.

References

- R. M. Donlan, Biofilm Formation: A Clinically Relevant Microbiological Process, *Clin. Infect. Dis.*, 2001, **33**(8), 1387–1392, DOI: [10.1086/322972](https://doi.org/10.1086/322972).
- P. Jjemba, W. Johnson, Z. Bukhari and M. LeChevallier, Review of the Leading Challenges in Maintaining Reclaimed Water Quality during Storage and Distribution, *J. Water Reuse Desalin.*, 2014, **4**(4), 209, DOI: [10.2166/wrd.2014.001](https://doi.org/10.2166/wrd.2014.001).
- H. F. Ridgway and B. H. Olson, Scanning Electron Microscope Evidence for Bacterial Colonization of a Drinking-Water Distribution System, *Appl. Environ. Microbiol.*, 1981, **41**(1), 274–287.
- M. W. Cowle, A. O. Babatunde, W. B. Rauen, B. N. Bockelmann-Evans and A. F. Barton, Biofilm Development in Water Distribution and Drainage Systems: Dynamics and Implications for Hydraulic Efficiency, *Environ. Technol. Rev.*, 2014, **3**(1), 31–47, DOI: [10.1080/09593330.2014.923517](https://doi.org/10.1080/09593330.2014.923517).
- S. Liu, C. Gunawan, N. Barraud, S. A. Rice, E. J. Harry and R. Amal, Understanding, Monitoring, and Controlling Biofilm Growth in Drinking Water Distribution Systems, *Environ. Sci. Technol.*, 2016, 8954–8976, DOI: [10.1021/acs.est.6b00835](https://doi.org/10.1021/acs.est.6b00835).
- I. B. Beech and J. Sunner, Biocorrosion: Towards Understanding Interactions between Biofilms and Metals, *Curr. Opin. Biotechnol.*, 2004, **15**(3), 181–186, DOI: [10.1016/j.copbio.2004.05.001](https://doi.org/10.1016/j.copbio.2004.05.001).
- C. Otto, S. Zahn, F. Rost, P. Zahn, D. Jaros and H. Rohm, Physical Methods for Cleaning and Disinfection of Surfaces, *Food Eng. Rev.*, 2011, **3**(3–4), 171–188, DOI: [10.1007/s12393-011-9038-4](https://doi.org/10.1007/s12393-011-9038-4).
- N. G. Reed, The History of Ultraviolet Germicidal Irradiation for Air Disinfection, *Public Health Rep.*, 2010, **125**(1), 15–27, DOI: [10.1177/003335491012500105](https://doi.org/10.1177/003335491012500105).
- S. E. Beck, H. Ryu, L. A. Boczek, J. L. Cashdollar, K. M. Jeanis, J. S. Rosenblum, O. R. Lawal and K. G. Linden, Evaluating UV-C LED Disinfection Performance and Investigating Potential Dual-Wavelength Synergy, *Water Res.*, 2017, **109**, 207–216, DOI: [10.1016/j.watres.2016.11.024](https://doi.org/10.1016/j.watres.2016.11.024).
- C. Chatterley and K. Linden, Demonstration and Evaluation of Germicidal UV-LEDs for Point-of-Use Water Disinfection, *J. Water Health*, 2010, **8**(3), 479–486, DOI: [10.2166/wh.2010.124](https://doi.org/10.2166/wh.2010.124).
- K. G. Linden, N. Hull and V. Speight, Thinking Outside the Treatment Plant: UV for Water Distribution System Disinfection, *Acc. Chem. Res.*, 2019, **52**(5), 1226–1233, DOI: [10.1021/acs.accounts.9b00060](https://doi.org/10.1021/acs.accounts.9b00060).
- R. P. Sinha and D.-P. Häder, UV-Induced DNA Damage and Repair: A Review, *Photochem. Photobiol. Sci.*, 2002, **1**(4), 225–236, DOI: [10.1039/b201230h](https://doi.org/10.1039/b201230h).
- A. Gupta, P. Avci, T. Dai, Y.-Y. Huang and M. R. Hamblin, Ultraviolet Radiation in Wound Care: Sterilization and Stimulation, *Adv. Wound Care*, 2013, **2**(8), 422–437, DOI: [10.1089/wound.2012.0366](https://doi.org/10.1089/wound.2012.0366).
- E. C. Friedberg, G. C. Walker, W. Siede, R. D. Wood, R. A. Schultz and T. Ellenberger, *DNA Repair and Mutagenesis*, ASM Press, Washington, DC, USA, 2005, DOI: [10.1128/9781555816704](https://doi.org/10.1128/9781555816704).
- M. Banas, M. Crawford, D. Ruby, M. Ross, J. Nelson, A. Allerman and R. Boucher, *Final LDRD Report :Ultraviolet Water Purification Systems for Rural Environments and Mobile Applications*, Albuquerque, NM, and Livermore, CA (United States), 2005, DOI: [10.2172/876370](https://doi.org/10.2172/876370).
- M. A. S. Ibrahim, J. MacAdam, O. Autin and B. Jefferson, Evaluating the Impact of LED Bulb Development on the Economic Viability of Ultraviolet Technology for Disinfection, *Environ. Technol.*, 2014, **35**(4), 400–406, DOI: [10.1080/09593330.2013.829858](https://doi.org/10.1080/09593330.2013.829858).
- G. Y. Lui, D. Roser, R. Corkish, N. Ashbolt, P. Jagals and R. Stuetz, Photovoltaic Powered Ultraviolet and Visible Light-Emitting Diodes for Sustainable Point-of-Use Disinfection of



- Drinking Waters, *Sci. Total Environ.*, 2014, **493**, 185–196, DOI: [10.1016/j.scitotenv.2014.05.104](https://doi.org/10.1016/j.scitotenv.2014.05.104).
- 18 Y. Muramoto, M. Kimura and S. Nouda, Development and Future of Ultraviolet Light-Emitting Diodes: UV-LED Will Replace the UV Lamp, *Semicond. Sci. Technol.*, 2014, **29**(8), 084004, DOI: [10.1088/0268-1242/29/8/084004](https://doi.org/10.1088/0268-1242/29/8/084004).
- 19 O. Autin, C. Romelot, L. Rust, J. Hart, P. Jarvis, J. MacAdam, S. A. Parsons and B. Jefferson, Evaluation of a UV-Light Emitting Diodes Unit for the Removal of Micropollutants in Water for Low Energy Advanced Oxidation Processes, *Chemosphere*, 2013, **92**(6), 745–751, DOI: [10.1016/j.chemosphere.2013.04.028](https://doi.org/10.1016/j.chemosphere.2013.04.028).
- 20 J. Chen, S. Loeb and J.-H. Kim, LED Revolution: Fundamentals and Prospects for UV Disinfection Applications, *Environ. Sci.: Water Res. Technol.*, 2017, **3**(2), 188–202, DOI: [10.1039/C6EW00241B](https://doi.org/10.1039/C6EW00241B).
- 21 J. Wu, M. Cao, D. Tong, Z. Finkelstein and E. M. V. Hoek, A Critical Review of Point-of-Use Drinking Water Treatment in the United States, *npj Clean Water*, 2021, **4**(1), 40, DOI: [10.1038/s41545-021-00128-z](https://doi.org/10.1038/s41545-021-00128-z).
- 22 E. L. Cates and H. Torkzadeh, Can Incorporation of UVC LEDs into Showerheads Prevent Opportunistic Respiratory Pathogens? – Microbial Behavior and Device Design Considerations, *Water Res.*, 2020, **168**, 115163, DOI: [10.1016/j.watres.2019.115163](https://doi.org/10.1016/j.watres.2019.115163).
- 23 M. Lanzarini-Lopes, B. Cruz, S. Garcia-Segura, A. Alum, M. Abbaszadegan and P. Westerhoff, Nanoparticle and Transparent Polymer Coatings Enable UV-C Side-Emission Optical Fibers for Inactivation of Escherichia Coli in Water, *Environ. Sci. Technol.*, 2019, **53**(18), 10880–10887, DOI: [10.1021/acs.est.9b01958](https://doi.org/10.1021/acs.est.9b01958).
- 24 M. Lanzarini-Lopes, Z. Zhao, F. Perreault, S. Garcia-Segura and P. Westerhoff, Germicidal Glowsticks: Side-Emitting Optical Fibers Inhibit Pseudomonas Aeruginosa and Escherichia Coli on Surfaces, *Water Res.*, 2020, **184**, 116191, DOI: [10.1016/j.watres.2020.116191](https://doi.org/10.1016/j.watres.2020.116191).
- 25 K. G. Linden, N. Hull and V. Speight, Thinking Outside the Treatment Plant: UV for Water Distribution System Disinfection: Published as Part of the Accounts of Chemical Research Special Issue “Water for Two Worlds: Urban and Rural Communities”, *Acc. Chem. Res.*, 2019, **52**, 1226–1233, DOI: [10.1021/acs.accounts.9b00060](https://doi.org/10.1021/acs.accounts.9b00060).
- 26 P. H. Quek and J. Hu, Indicators for Photoreactivation and Dark Repair Studies Following Ultraviolet Disinfection, *J. Ind. Microbiol. Biotechnol.*, 2008, **35**(6), 533–541, DOI: [10.1007/s10295-008-0314-0](https://doi.org/10.1007/s10295-008-0314-0).
- 27 H. Torkzadeh, K. R. Zodrow, W. C. Bridges and E. L. Cates, Quantification and Modeling of the Response of Surface Biofilm Growth to Continuous Low Intensity UVC Irradiation, *Water Res.*, 2021, **193**, 116895, DOI: [10.1016/j.watres.2021.116895](https://doi.org/10.1016/j.watres.2021.116895).
- 28 M. Hu and J. B. Gurtler, Selection of Surrogate Bacteria for Use in Food Safety Challenge Studies: A Review, *J. Food Prot.*, 2017, **80**(9), 1506–1536, DOI: [10.4315/0362-028X.JFP-16-536](https://doi.org/10.4315/0362-028X.JFP-16-536).
- 29 Y. Cheng, H. Chen, L. A. Sánchez Basurto, V. V. Protasenko, S. Bharadwaj, M. Islam and C. I. Moraru, Inactivation of Listeria and E. Coli by Deep-UV LED: Effect of Substrate Conditions on Inactivation Kinetics, *Sci. Rep.*, 2020, **10**(1), 3411, DOI: [10.1038/s41598-020-60459-8](https://doi.org/10.1038/s41598-020-60459-8).
- 30 R. A. Andersen and M. Kawachi, Microalgae Isolation Techniques, *Algal Cult. Tech.*, 2005, vol. 83, p. 592.
- 31 A. Green, V. Popović, J. Pierscianowski, M. Biancanello, K. Warriner and T. Koutchma, Inactivation of Escherichia Coli, Listeria and Salmonella by Single and Multiple Wavelength Ultraviolet-Light Emitting Diodes, *Innovative Food Sci. Emerging Technol.*, 2018, **47**, 353–361, DOI: [10.1016/j.ifset.2018.03.019](https://doi.org/10.1016/j.ifset.2018.03.019).
- 32 P. O. Nyangaresi, Y. Qin, G. Chen, B. Zhang, Y. Lu and L. Shen, Effects of Single and Combined UV-LEDs on Inactivation and Subsequent Reactivation of E. Coli in Water Disinfection, *Water Res.*, 2018, **147**, 331–341, DOI: [10.1016/j.watres.2018.10.014](https://doi.org/10.1016/j.watres.2018.10.014).
- 33 D. K. Kim, S. J. Kim and D. H. Kang, Bactericidal Effect of 266 to 279 Nm Wavelength UVC-LEDs for Inactivation of Gram Positive and Gram Negative Foodborne Pathogenic Bacteria and Yeasts, *Food Res. Int.*, 2017, **97**, 280–287, DOI: [10.1016/j.foodres.2017.04.009](https://doi.org/10.1016/j.foodres.2017.04.009).
- 34 K. Oguma, H. Katayama, H. Mitani, S. Morita, T. Hirata and S. Ohgaki, Determination of Pyrimidine Dimers in Escherichia Coli and Cryptosporidium Parvum during UV Light Inactivation, Photoreactivation, and Dark Repair, *Appl. Environ. Microbiol.*, 2001, **67**(10), 4630–4637, DOI: [10.1128/AEM.67.10.4630-4637.2001](https://doi.org/10.1128/AEM.67.10.4630-4637.2001).
- 35 J. L. Zimmer and R. M. Slawson, Potential Repair of Escherichia Coli DNA Following Exposure to UV Radiation from Both Medium- and Low-Pressure UV Sources Used in Drinking Water Treatment, *Appl. Environ. Microbiol.*, 2002, **68**(7), 3293–3299, DOI: [10.1128/aem.68.7.3293-3299.2002](https://doi.org/10.1128/aem.68.7.3293-3299.2002).
- 36 P. H. Quek, J. Y. Hu, X. N. Chu, Y. Y. Feng and X. L. Tan, Photoreactivation of Escherichia Coli Following Medium-Pressure Ultraviolet Disinfection and Its Control Using Chloramination, *Water Sci. Technol.*, 2006, **53**(6), 123–129, DOI: [10.2166/wst.2006.184](https://doi.org/10.2166/wst.2006.184).
- 37 J. R. S. Brownson, Laws of Light, in *Solar Energy Conversion Systems*, Elsevier, 2014, pp. 41–66, DOI: [10.1016/B978-0-12-397021-3.00003-X](https://doi.org/10.1016/B978-0-12-397021-3.00003-X).
- 38 A. Argyraki, M. Markqvart, A. Nielsen, T. Bjørnsholt, L. Bjørndal and P. M. Petersen, Comparison of UVB and UVC Irradiation Disinfection Efficacies on Pseudomonas Aeruginosa (P. aeruginosa) Biofilm, ed. J. Popp, V. V. Tuchin, D. L. Matthews and F. S. Pavone, 2016, p. 988730, DOI: [10.1117/12.2225597](https://doi.org/10.1117/12.2225597).
- 39 J. Bak, S. D. Ladefoged, M. Tvede, T. Begovic and A. Gregersen, Dose Requirements for UVC Disinfection of Catheter Biofilms, *Biofouling*, 2009, **25**(4), 289–296, DOI: [10.1080/08927010802716623](https://doi.org/10.1080/08927010802716623).
- 40 K. Kollu and B. Örmeci, Effect of Particles and Bioflocculation on Ultraviolet Disinfection of Escherichia Coli, *Water Res.*, 2012, **46**(3), 750–760, DOI: [10.1016/j.watres.2011.11.046](https://doi.org/10.1016/j.watres.2011.11.046).



- 41 J. Li, K. Hirota, H. Yumoto, T. Matsuo, Y. Miyake and T. Ichikawa, Enhanced Germicidal Effects of Pulsed UV-LED Irradiation on Biofilms, *J. Appl. Microbiol.*, 2010, **109**(6), 2183–2190, DOI: [10.1111/j.1365-2672.2010.04850.x](https://doi.org/10.1111/j.1365-2672.2010.04850.x).
- 42 C. N. Pace, F. Vajdos, L. Fee, G. Grimsley and T. Gray, How to Measure and Predict the Molar Absorption Coefficient of a Protein, *Protein Sci.*, 1995, **4**(11), 2411–2423, DOI: [10.1002/pro.5560041120](https://doi.org/10.1002/pro.5560041120).
- 43 C. M. Stoscheck, [6] Quantitation of Protein, *Methods Enzymol.*, 1990, **182**, 50–68, DOI: [10.1016/0076-6879\(90\)82008-P](https://doi.org/10.1016/0076-6879(90)82008-P).
- 44 G.-Q. Li, W.-L. Wang, Z.-Y. Huo, Y. Lu and H.-Y. Hu, Comparison of UV-LED and Low Pressure UV for Water Disinfection: Photoreactivation and Dark Repair of Escherichia Coli, *Water Res.*, 2017, **126**, 134–143, DOI: [10.1016/j.watres.2017.09.030](https://doi.org/10.1016/j.watres.2017.09.030).
- 45 D.-K. Kim and D.-H. Kang, Elevated Inactivation Efficacy of a Pulsed UVC Light-Emitting Diode System for Foodborne Pathogens on Selective Media and Food Surfaces, *Appl. Environ. Microbiol.*, 2018, **84**(20), DOI: [10.1128/AEM.01340-18](https://doi.org/10.1128/AEM.01340-18).
- 46 S. L. Gora, K. D. Rauch, C. C. Ontiveros, A. K. Stoddart and G. A. Gagnon, Inactivation of Biofilm-Bound Pseudomonas Aeruginosa Bacteria Using UVC Light Emitting Diodes (UVC LEDs), *Water Res.*, 2019, **151**, 193–202, DOI: [10.1016/j.watres.2018.12.021](https://doi.org/10.1016/j.watres.2018.12.021).
- 47 B. Ma, S. Seyedi, E. Wells, D. McCarthy, N. Crosbie and K. G. Linden, Inactivation of Biofilm-Bound Bacterial Cells Using Irradiation across UVC Wavelengths, *Water Res.*, 2022, **217**, 118379, DOI: [10.1016/j.watres.2022.118379](https://doi.org/10.1016/j.watres.2022.118379).

